Mon. Not. R. Astron. Soc. **351,** 552–568 (2004) doi:10.1111/j.1365-2966.2004.07799.x

Large-scale wind structures in OB supergiants: a search for rotationally modulated Hα variability

T. Morel,[1,2]⋆ S. V. Marchenko,[3] A. K. Pati,[4] K. Kuppuswamy,[5] M. T. Carini,[3] E. Wood[3] and R. Zimmerman[3]

[1]*Istituto Nazionale di Astrofisica, Osservatorio Astronomico di Palermo G. S. Vaiana, Piazza del Parlamento 1, I-90134 Palermo, Italy*
[2]*Inter-University Centre for Astronomy and Astrophysics (IUCAA), Post Bag 4, Ganeshkhind, Pune, 411 007, India*
[3]*Department of Physics and Astronomy, Western Kentucky University, 1 Big Red Way, Bowling Green, KY 42101–3576, USA*
[4]*Indian Institute of Astrophysics (IIAP), III block, Koramangala, Bangalore, India*
[5]*Vainu Bappu Observatory, Indian Institute of Astrophysics (IIAP), Kavalur, Alangayam 635 701 India*

Accepted 2004 March 3. Received 2004 February 27; in original form 2003 December 9

ABSTRACT

We present the results of a long-term monitoring campaign of the Hα line in a sample of bright OB supergiants (O7.5–B9) which aims at detecting rotationally modulated changes potentially related to the existence of large-scale wind structures. A total of 22 objects were monitored during 36 nights spread over six months in 2001–2002. Coordinated broad-band photometric observations were also obtained for some targets. Conspicuous evidence for variability in Hα is found for the stars displaying a feature contaminated by wind emission. Most changes take place on a daily time-scale, although hourly variations are also occasionally detected. Convincing evidence for a cyclical pattern of variability in Hα has been found in two stars: HD 14134 and HD 42087. Periodic signals are also detected in other stars, but independent confirmation is required. Rotational modulation is suggested from the similarity between the observed recurrence time-scales (in the range 13–25 d) and estimated periods of stellar rotation. We call attention to the atypical case of HD 14134, which exhibits a clear 12.8-d periodicity, both in the photometric and in the spectroscopic data sets. This places this object among a handful of early-type stars where one may observe a clear link between extended wind structures and photospheric disturbances. Further modelling may test the hypothesis that azimuthally-extended wind streams are responsible for the patterns of spectral variability in our target stars.

Key words: stars: early-type – stars: emission-line, Be – stars: rotation – supergiants – stars: winds, outflows.

1 INTRODUCTION

One of the major legacies of the *International Ultraviolet Explorer* (*IUE*) was to establish the ubiquity of ultraviolet (UV) line-profile variability in OB stars. The pattern of variability predominantly consists of extra absorption features (the so-called 'discrete absorption components', hereafter DACs) moving blueward across the (unsaturated) absorption troughs of P Cygni lines (e.g. Kaper et al. 1996). The repetitive nature of DACs and the fact that the recurrence time-scale is commensurate with the (otherwise ill-defined) stellar rotational period suggest that rotation plays a key role in inducing the patterns of variability (e.g. Kaper et al. 1999). UV time series with a long temporal baseline (i.e. sampling several rotational periods) have revealed that OB stars exhibit a great diversity of behaviours that cannot always be strictly related to the stellar rotation period (e.g. Howarth, Prinja & Massa 1995; Prinja, Massa & Fullerton 1995, 2002). Nevertheless, this global phenomenon has been successfully interpreted in several cases in the framework of a model in which the changes are caused by the rotational modulation of large-scale, azimuthally-extended wind streams (e.g. Fullerton et al. 1997).

The hydrodynamical simulations of Cranmer & Owocki (1996) suggest that large-scale photospheric perturbations (e.g. bright 'spots' causing a local enhancement of the radiative driving force) may lead to the development of these structures. Although the underlying physical mechanism remains elusive, pulsational instability can be invoked as a trigger of the wind variability (e.g. Fullerton, Gies & Bolton, 1996). Large-scale or 'surface' magnetic field structures could be a viable alternative in view of the growing

⋆E-mail: morel@astropa.unipa.it

evidence for (weak) magnetic fields in OB stars (e.g. Henrichs, Neiner & Geers 2003). Photospheric perturbations arising from these two phenomena are likely to have a significant impact on the global wind morphology (e.g. ud-Doula & Owocki 2002).

With the demise of *IUE*, further progress on this issue is likely to stem in the foreseeable future from time-resolved studies of line variability in the optical. First, intensive UV observations have been carried out over several rotation periods for few stars (Massa et al. 1995; Prinja et al. 1998; de Jong et al. 2001). For practical reasons, an optical survey is much more amenable at collecting high-quality observations covering several cycles for a large, representative sample of OB stars. Secondly, in contrast to the UV resonance lines, optical recombination lines are (at least partly) formed in OB supergiants in the dense, strongly accelerating part of the outflow close to the stellar core. In virtue of their density-squared dependence, they are good probes of the large density gradients expected to prevail in the corotating interaction regions (Cranmer & Owocki 1996). Revealing a cyclical pattern of variability in these lines would give further credence to the idea that the origin of anisotropic outflows in OB stars is deep-seated and causally linked to processes taking place at the stellar photosphere. Here we discuss the temporal behaviour of Hα, which is typically formed at $r \sim 1.5\ R_\star$ in O-type stars (e.g. Prinja, Fullerton & Crowther 1996). Although the line-formation region is likely to be more extended in B-type supergiants, this transition still probes the few inner radii of the stellar wind.

Previous surveys have been very useful in documenting Hα line-profile variability in OB stars (e.g. Ebbets 1982), but frequently suffered from a poor temporal sampling hampering the study of the line-profile variations on a rotational time-scale (up to several weeks in the case of B supergiants). Despite the persistent and numerous searches for optical line-profile variability in OB stars, evidence for rotational modulation has been found in only few cases (e.g. Moffat & Michaud 1981; Kaper et al. 1997, 1998). In the UV and optical domains, the time-scales associated with the changes are often identical, within the uncertainties (e.g. Howarth, Prinja & Massa 1995; Kaper et al. 1999; de Jong et al. 2001; Kaufer, Prinja & Stahl 2002). This suggests that Hα variability and DACs diagnose the same underlying physical phenomenon.

The long-term monitoring of the Hα line presented in this paper aims at better establishing the incidence of rotationaly modulated variability in OB supergiants. To potentially link the photospheric and wind activity, coordinated broad-band photometic observations were also carried out for a subset of this sample. Our survey primarily targets early B-type stars and can thus be regarded as complementary to others that concentrate on O-type (Kaper 1998; Kaper et al. 1998) or late B- to early A-type supergiants (Kaufer et al. 1996). The results presented in the following supersede previous preliminary reports (Morel et al. 2004a,b).

2 TARGET SELECTION AND TEMPORAL SAMPLING OF THE OBSERVATIONS

Our targets are drawn from a magnitude-limited ($V < 7.5$) sample of early-type supergiants (O7.5–B9) with evidence for an emission-like Hα profile or, in the case of stars with an absorption feature, for previous claims of a wind-related variability (e.g. filling-in of the profile). Known close binaries were discarded from this list in order to avoid contamination from the wind collision effects (e.g. Thaller et al. 2001). The wide binary orbit of HD 37742 rules out the formation of a bow shock created from the interaction with an O-type companion (Hummel et al. 2000). In our data only HD 13854 and HD 47240 present significant velocity variations of the photospheric He I λ6678.15 line which might be attributed to binary motion (see below). Dwarfs and giant stars were not included in this list, as Hα is of photospheric origin in the vast majority of these objects. The only exception was the O7.5 giant HD 24912 (ξ Per) because of previous claims of a cyclical, wind-related pattern of variability in Hα (Kaper et al. 1997; de Jong et al. 2001). For the other stars in our list, no clear evidence for cyclical line-profile variations in optical wind lines was found prior to our survey. Some physical parameters of our programme stars are given in Table 1.

The basic requirement of this survey was to achieve a time sampling allowing a proper assessment of the variability pattern on a rotational time-scale (typically one to two weeks). Although the rotational periods of our programme stars are unknown, the critical and projected rotational velocities can be used, along with the estimates of the stellar radii, to set a lower and an upper limit on this quantity. As can be seen in Table 2, the estimated rotational periods span a wide range of values (1.2–144 d). Our 22 programme stars were monitored during a total of 36 nights spread over six months, with one to two spectra obtained every night. This long-term monitoring was necessary to cover at least one rotational cycle for the slowly rotating objects. We also obtained intranight observations, expecting significant hourly changes in some cases (e.g. HD 24912). In general, this temporal sampling appears to be adequate for our purpose (see Table 3). For five stars, however, the observations were too sparse to reliably investigate a potential cyclical behaviour (HD 14818, HD 21291, HD 119608, HD 151804 and HD 152236). No period search was performed in this case (see Section 5.2), but a qualitative description of the changes is presented in Section 4.

3 OBSERVATIONS AND REDUCTION PROCEDURE

3.1 Spectroscopy

Our observations were obtained during four observing runs conducted between 2001 November and 2002 May at the 40-inch telescope of the Vainu Bappu Observatory (VBO), Kavalur, India. The spectograph was equipped with a TK 1k CCD chip. We used the 651 l mm^{-1} grating blazed in the first order at 7500 Å, which yields at Hα a reciprocal dispersion of 1.45 Å pixel^{-1} (we used a 120-μm wide slit), thus covering the spectral region 5810–7205 Å. The slit of the spectrograph was rotated for HD 37742 in order to avoid contamination from the visual companion. The speckle interferometric observations of Mason et al. (1998) exclude the existence in HD 24912, HD 30614 and HD 151804 of bright ($\Delta m \lesssim 3$ mag), close companions ($0.035 \lesssim \rho \lesssim 1.5$ arcsec). Apart from HD 37742, a search in the *Hipparcos* data base reveals only one star in our sample with a close visual component (HD 42087: $\Delta H_{\rm p} = 2.58$ mag and $\rho = 0.6$ arcsec).

The IRAF[1] tasks were used to carry out standard reduction procedures (i.e. bias subtraction, flat-fielding, extraction of the spectra, and wavelength calibration). Spectra of FeNe lamps were taken immediately before and/or after the stellar exposure. The spectra were subsequently put in the heliocentric velocity frame. The Hα line profiles were found to be significantly affected by telluric lines, as the observations were often carried out under unfavourable atmospheric

[1] IRAF is distributed by the National Optical Astronomy Observatories, operated by the Association of Universities for Research in Astronomy, Inc., under cooperative agreement with the National Science Foundation.

Table 1. Physical parameters of the programme stars: spectral types and wind terminal velocities, v_∞, from Howarth et al. (1997) and references therein; effective temperatures from the calibration of Humphreys & MacElroy (1984); stellar luminosities calculated from the calibrated M_V values and bolometric corrections of Humphreys & MacElroy (1984); stellar masses from Lamers (1981) – the numbers in brackets are estimates based on his values for similar spectral types and luminosity classes (this source was used because it constitutes the most homogeneous data base, but we warn the reader that these values may be significantly revised; see, for example, Herrero, Puls & Najarro 2002); stellar radii determined from the effective temperatures and luminosities; mass-loss rates, $\dot{M}$, calculated from the empirical relation for galactic OBA supergiants of Lamers & Cassinelli (1996) – the value for HD 24912 was derived from their relation for giants; projected rotational velocities, $v \sin i$, from Howarth et al. (1997); critical rotational velocities, $v_{\rm crit}$, calculated following Howarth & Prinja (1989) – the values in brackets are poorly determined because of an uncertain stellar mass.

Name	V (mag)	Spectral type	$T_{\rm eff}$ (K)	$\log(L_\star/{\rm L}_\odot)$	$M_\star$ ($M_\odot$)	$R_\star$ ($R_\odot$)	$\dot{M}$ (10^{-6} $M_\odot$ yr^{-1})	v_∞ (km s^{-1})	$v \sin i$ (km s^{-1})	$v_{\rm crit}$ (km s^{-1})
HD 13854	6.49	B1 Iab	20 260	5.18	(22)	32	0.76	920	97	(328)
HD 14134 (V520 Per)	6.55	B3 Ia	16 300	5.24	24	52	1.45	465	66	265
HD 14818 (10 Per)	6.26	B2 Ia	18 000	5.40	(30)	52	2.13	565	82	(293)
HD 21291	4.25	B9 Ia[a]	10 250	4.86	19	85			30[b]	195
HD 24398 (ζ Per)	2.88	B1 Ib	20 260	4.90	21	23	0.23	1295	67	396
HD 24912 (ξ Per)	4.04	O7.5 III (n)((f))	35 400	5.40	28	13	0.22	2330	213	550
HD 30614 (α Cam)	4.30	O9.5 Ia	29 900	5.86	40	32	5.03	1590	129	350
HD 31327	6.09	B2 Ib	18 000	4.76	(20)	25			60	(377)
HD 37128 (ϵ Ori)	1.70	B0 Ia	28 600	5.78	38	32	3.15	1910	91	362
HD 37742 (ζ Ori A)	1.7	O9.7 Ib	29 250	5.40	25	20	1.05	1860	124	421
HD 38771 (κ Ori)	2.04	B0.5 Ia	23 100	5.50	35	35	1.37	1525	83	379
HD 41117 (χ^2 Ori)	4.64	B2 Ia	18 000	5.40	32	52	2.36	510	72	305
HD 42087 (3 Gem)	5.76	B2.5 Ib	17 150	4.72	(19)	26	0.20	735	71	(359)
HD 43384 (9 Gem)	6.29	B3 Iab	16 300	4.88	(22)	35	0.30	760	59	(331)
HD 47240	6.18	B1 Ib	20 260	4.90	(21)	23	0.31	960	103	(396)
HD 52382	6.51	B1 Ib	20 260	4.90	(21)	23	0.33	900	74	(396)
HD 53138 (o^2 CMa)	3.00	B3 Ia	16 300	5.24	23	52	0.78	865	58	258
HD 58350 (η CMa)	2.40	B5 Ia	13 700	5.02	20	58	0.91	320	50	238
HD 91316 (ρ Leo)	3.84	B1 Iab	20 260	5.18	22	32	0.63	1110	75	328
HD 119608	7.50	B1 Ib	20 260	4.90	(21)	23	0.34	880	74	(396)
HD 151804	5.24	O8 Iaf	33 500	6.06	(60)	32	11.3	1445	104	(416)
HD 152236 (ζ^1 Sco)	4.77	B0.5 Ia+	19 700[c]	6.05[c]	(35)	91[c]	5.36	390	74	(99)

Notes. [a]From the SIMBAD data base. [b]From Abt, Levato & Grosso (2002). [c]From Rivinius et al. (1997).

conditions (e.g. high humidity). Therefore, we have obtained spectra of the rapid rotator HD 65810 (A1 V) to create a library of telluric lines that would be used on the target stars. Because this procedure proved unsatisfactory, we used instead the high-resolution telluric spectrum of Hinkle et al. (2000) degraded to our resolution. The water vapour lines in the pseudo-continuum regions around Hα were interactively shifted and scaled with the IRAF task TELLURIC until the residuals between the observed spectra and the template telluric spectrum were minimized. The spectra were finally continuum-rectified by fitting a low-order spline3 polynomial to fixed line-free spectral regions on both sides of Hα. We generally obtained three consecutive exposures to allow a more robust rectification of the spectra and filtering of cosmic ray events. Any individual exposure with evidence for an imperfect continuum normalization was excluded during the co-adding operation. The typical signal-to-noise (S/N) ratio at Hα in the combined spectrum is quoted for each star in Table 3, and lies in the range 125–335 per pixel in the continuum. Large velocity variations of the photospheric He I λ6678 line, which might arise from binary motion, were found in HD 13854 and HD 47240 ($\sigma \sim 15$ and 30 km s^{-1}, respectively). The spectra were hence realigned and put in the same reference frame. The remaining stars may have companions (e.g. HD 37742), but the radial velocity variations are small, i.e. comparable to the typical uncertainties in the wavelength calibration ($\sim$5 km s^{-1}). Hence, all the discussed spectral variations should be intrinsic to the star.

3.2 Photometry

Coordinated *B*- and *I*-band (Johnson) photometric observations were carried out with the 24-inch telescope of the Bell Observatory operated by the Western Kentucky University (USA). Six stars were observed during seven nights in 2002 January, February and

Table 2. Summary of period search (all periods in d): $\mathcal{P}_{\rm min}$ and $\mathcal{P}_{\rm max}$, lower and upper limits on the stellar rotational period (determined from the critical and projected rotational velocities, along with an estimate of the stellar radius); $\mathcal{P}$(phot), periodicities in the *Hipparcos* data (var, stars displaying photometric variability but without evidence for periodicity; non-var, stars without significant variability) – the light curves are shown in Fig. 2 (and in Fig. 4 for HD 14134); $\mathcal{P}$(literature), literature values for the periodicities in Hα (Kaper et al. 1997, 1998; de Jong et al. 2001; Markova 2002). The numbers in italics refer to the periodicities in the UV wind line profiles (Kaper et al. 1999; de Jong et al. 2001). Multiple values refer to periods derived at different epochs. Numbers in brackets indicate that the periodicity found is longer that the time-span of the *IUE* observations. For the Hα periodicities derived from our observations, $\mathcal{P}$(Hα), '2D' and 'EW' indicate that the period is present in the Hα pixel-to-pixel or EW time series, respectively.

Name	$\mathcal{P}_{\rm min}$	$\mathcal{P}_{\rm max}$	$\mathcal{P}$(phot)	$\mathcal{P}$(literature)[a]	$\mathcal{P}$(Hα)[b]
HD 13854	(4.9)	16.5	5.644		1.047 (EW)
HD 14134 (V520 Per)	10	40.1	12.823		22.2 (2D), 12.5 (2D and EW)
HD 14818 (10 Per)	(8.9)	31.8	2.754		No period search performed
HD 21291	22	144	26.76	[1,2,3]	No period search performed
HD 24398 (ζ Per)	2.9	17.3	Non-var		No periods found
HD 24912 (ξ Per)	1.2	3.17	Non-var	2.1 $\pm$ 0.1, 1.96$\pm$0.11, 2.086 [4,5,6]	2.197 ? (2D and EW)
				1.9 $\pm$ 0.3, 1.0 $\pm$ 0.1, 2.0 $\pm$ 0.2	
HD 30614 (α Cam)	4.6	12.5	Var	$\sim$5.6, $\sim$7, $\sim$10 [5,6,7,8,9]	No periods found
HD 31327	(3.3)	20.8	Non-var		No periods found
HD 37128 (ϵ Ori)	4.4	17.6	Var	[8,10]	18.2, 0.781 (both 2D)
HD 37742 (ζ Ori A)	2.3	7.97	1.407	$\sim$6 [5,6,8]	$\gtrsim$80 (2D), 50 (2D), 13.3 (EW)
				(6.3$\pm$2.1), (6.1$\pm$2.7)	1.136 (2D), 0.877 (2D)
HD 38771 (κ Ori)	4.7	21.4	Var	[7,8,11]	4.76, 1.047 (both 2D)
HD 41117 (χ^2 Ori)	8.6	36.3	2.869	[1,8,12,13]	$\gtrsim$80 (2D), 40 (2D and EW), 0.957 (2D), 0.922 (2D)
HD 42087 (3 Gem)	(3.7)	18.5	6.807		25 (2D and EW)
HD 43384 (9 Gem)	(5.3)	29.7	13.7		No periods found
HD 47240	(2.9)	11.3	2.7424		No periods found
HD 52382	(2.9)	15.7	Var		No periods found
HD 53138 (o^2 CMa)	10	45.7	Var	[8,14]	No periods found
HD 58350 (η CMa)	12	58.2	Var	[8]	No periods found
HD 91316 (ρ Leo)	4.9	21.3	Var[c]	[12,13,15]	No periods found
HD 119608	(2.9)	15.7	Non-var		No period search performed
HD 151804	(3.9)	15.5	Non-var[d]	7.3 [6,16]	No period search performed
HD 152236 (ζ^1 Sco)	(46)	62.3	Var[e]	[17,18]	No period search performed

Notes. [a]The numbers in square brackets refer to previous investigations of Hα variability in our programme stars: 1, Rosendhal (1973); 2, Denizman & Hack (1988); 3, Zeinalov & Rzaev (1990); 4, de Jong et al. (2001); 5, Kaper et al. (1997); 6, Kaper et al. (1998); 7, Ebbets (1980); 8, Ebbets (1982); 9, Markova (2002); 10, Cherrington (1937); 11, Rusconi et al. (1980); 12, Underhill (1960); 13, Underhill (1961); 14, van Helden (1972); 15, Smith & Ebbets (1981); 16, Prinja et al. (1996); 17, Sterken & Wolf (1978); 18, Rivinius et al. (1997).
[b]The typical uncertainties for the quoted periods have been derived from the FWHM of the peaks in the PS and amount to: 20–30 d ($\mathcal{P} \gtrsim 50$ d); 1–4 d ($10 \lesssim \mathcal{P}$ (d) $\lesssim 25$); 0.01–0.2 d ($1 \lesssim \mathcal{P}$ (d) $\lesssim 5$); and 0.01 d ($\mathcal{P} \lesssim 1$ d). [c]Multiperiodic variable according to Koen (2001). [d]Photometric variable according to Balona (1992), and references therein. [e]Irregular, multiperiodic photometric variable (Sterken et al. 1997).

April: HD 13854, HD 14134, HD 14818, HD 42087, HD 47240 and HD 52382. A typical observation (repeated up to three times per night) comprises up to 10 short-exposure (1–10 s) CCD images of the target and the surrounding field (0.53 arcsec pixel^{-1} scale, providing a 4.4 $\times$ 6.6 arcmin^2 field).

The standard processing routines were performed with IRAF tasks and included bias and flat-field correction, followed by measurements of all available comparison stars in the fields surrounding the targets. Pre-selection of appropriate comparison stars was based on their brightness and non-variability. All the differential measurements performed on the stars from individual frames were combined into normal observation, thus producing one to three data points per night for each star. This resulted in overall accuracy $\sim$0.01 mag per data point for each comparison star. This relatively low accuracy was mainly dictated by the lack of appropriately bright comparison stars, the problem being especially acute for HD 14818, HD 42087 and HD 47240. For HD 42087, in particular, there was only one very faint comparison star in the field, resulting in a much lower accuracy ($\sim$0.02 mag). These data are not discussed in the following.

4 OVERVIEW OF THE SURVEY AND QUANTITATIVE ANALYSIS

The Hα time series are shown in Fig. 1, along with the temporal variance spectra (TVS; Fullerton et al. 1996). As can be seen, all stars display significant variability across most of the Hα profile (the extent of the variability in velocity space is well correlated with the wind terminal velocity: $\Delta v \sim \pm 0.3 v_\infty$). One can note that morphological evidence for a Hα feature partly formed in the outflow (i.e. a line profile clearly departing from a pure photospheric one) is systematically accompanied by much more prominent changes. The detected variability is qualitatively similar to the cases reported by Ebbets (1982). Noteworthy is the emission-like episode experienced by HD 14134 and HD 43384. The dramatic variations previously reported in HD 21291 (Denizman & Hack 1988; Zeinalov & Rzaev 1990) and HD 91316 (Smith & Ebbets 1981) are not seen in our data.

Most changes take place on a daily time-scale, although significant hourly variations are sometimes observed. These subtle,

Table 3. Temporal sampling of the spectroscopic observations: N, total number of spectra obtained; ΔT, total time-span of the observations; Min(Δt), Mean(Δt) and Max(Δt), minimum, mean and maximum time intervals between consecutive spectra, respectively.

Name	Run[a]	No. nights	N	⟨S/N⟩	ΔT (d)	Min(Δt) (d)	Mean(Δt) (d)	Max(Δt) (d)
HD 13854	A,B,C	16	19	210	71.1	0.07	3.95	24.0
HD 14134 (V520 Per)	A,B,C	17	22	205	67.1	0.07	3.19	24.0
HD 14818 (10 Per)	C	7	7	170	12.0	0.93	2.01	4.06
HD 21291	C	7	7	190	8.01	0.93	1.33	2.97
HD 24398 (ζ Per)	A,B	9	13	305	38.8	0.07	3.24	24.9
HD 24912 (ξ Per)	A,B,C	17	23	250	75.8	0.07	3.45	26.0
HD 30614 (α Cam)	A,B,C	16	19	240	70.9	0.07	3.94	26.0
HD 31327	A,B	10	12	265	38.9	0.10	3.54	23.0
HD 37128 (ϵ Ori)	A,B,C,D	17	21	335	129	0.05	6.44	48.9
HD 37742 (ζ Ori A)	A,B,C,D	23	27	275	133	0.10	5.10	48.9
HD 38771 (κ Ori)	A,B,C,D	19	22	280	130	0.15	6.17	49.8
HD 41117 (χ^2 Ori)	A,B,C,D	22	25	220	131	0.11	5.44	49.9
HD 42087 (3 Gem)	A,B,C,D	20	20	210	135	0.86	7.09	49.8
HD 43384 (9 Gem)	A,C,D	17	17	220	133	0.87	8.29	51.9
HD 47240	A,C,D	16	16	195	133	0.91	8.85	51.9
HD 52382	A,C,D	17	17	180	164	0.85	10.2	56.0
HD 53138 (o^2 CMa)	A,B,C,D	20	22	230	164	0.10	7.79	50.9
HD 58350 (η CMa)	C,D	14	17	210	104	0.08	6.48	48.8
HD 91316 (ρ Leo)	A,B,C,D	19	20	200	162	0.07	8.50	48.8
HD 119608	C,D	7	7	135	104	1.09	17.3	55.9
HD 151804	D	7	7	125	42.0	0.99	6.99	30.9
HD 152236 (ζ^1 Sco)	D	6	6	165	42.0	1.02	8.39	31.0

[a] A, 2001 November 18–December 04; B, 2001 December 27–28; C, 2002 January 21–February 03; D, 2002 March 24–May 07.

short-term changes should be considered with some caution. In some cases, we cannot exclude the possibility that they largely arise from an imperfect continuum normalization and/or removal of telluric features (Section 3.1). To better assess the reality of these short-term variations, we use a 'quality flag' defined as the number of co-added consecutive exposures (indicated for each spectrum in Fig. 1). Hourly changes between spectra rated as '1' should be regarded with some suspicion (e.g. HD 14134), whereas they are very likely to be real between spectra rated as '3' (e.g. HD 37128). Our data support the hourly changes found in HD 38771 by Rusconi et al. (1980), but not the variations on a time-scale of 30 min reported for HD 53138 by van Helden (1972).

One should bear in mind that the observed variations in Hα may not be straightforwardly associated with wind activity. It is likely that time-dependent changes, possibly arising from pulsations, as commonly observed in early-type supergiants (e.g. Kaufer et al. 1997; de Jong et al. 1999), also affect the underlying photospheric profile. Although our modest spectral resolution precludes a detailed study, we choose to illustrate the temporal changes in photospheric lines by means of He I λ6678.[2] With the exception of HD 152236 which occasionally exhibits a P Cygni profile, this feature appears to be primarily of photospheric origin for all the stars in our sample. The changes affecting this line are generally significant (see Fig. 1), and are likely paralleled in the Hα photospheric component. Because of substantial pressure broadening in B-type supergiants, such variations will extend in velocity space well beyond the projected rotational velocity (e.g. Ryans et al. 2002). In many cases the observed He I λ6678 variability barely exceeds the detection thresholds, which prevents us from linking the patterns observed in Hα and He I λ6678. The limited spectral resolution also precludes a straightforward interpretation of the variability as arising either from a variable, incipient emission or from temporal fluctuations in the shape of the absorption profile (e.g. HD 31327). A direct comparison between the patterns of variability in He I λ6678 and Hα will be presented for two illustrative cases in Section 6.1.

To quantify the level of spectral and photometric variability, we define the two activity indices $a_{\rm phot}$ and $a_{\rm lpv}$ (Table 4). The former was calculated both from *Hipparcos* data and from our photometric observations, and is defined as $a^2_{\rm phot} = \sigma^2_{\rm obs} - \sigma^2_{\rm instr}$, where $\sigma_{\rm obs}$ and $\sigma_{\rm instr}$ are the scatter of the observations and the instrumental noise, respectively (see Marchenko et al. 1998). The spectral variability index, $a_{\rm lpv}$, is the fractional amplitude of the line-profile variations, i.e. the amplitude of the changes normalized by the strength of the feature (see equation 15 of Fullerton et al. 1996). This index was calculated both for Hα and for He I λ6678.

5 PERIOD SEARCH

We performed a period search analysis by calculating the power spectra (PS) using the technique of Scargle (1982) on: (i) the photometric *Hipparcos* data (our observations are not amenable to a period search); (ii) the pixel-to-pixel Hα time series; (iii) the equivalent widths (EWs) measured within fixed wavelength intervals encompassing the whole of Hα (*even* in the case of P Cygni profiles). Despite the fact that the EW and pixel-to-pixel line-profile variations are not, strictly speaking, two independent quantities, a period search in the two data sets is helpful in assessing the reality of the detected signals. Subsequent correction of the frequency spectrum by the CLEAN algorithm was performed in order to remove aliases and spurious features induced by the uneven spacing of the data in the time domain (Roberts, Lehár & Dreher 1987).

[2] We do not discuss the variations that may affect the potentially interesting He I λ5876 line because of difficulties in defining the neighbouring continuum, as well as edge effects.

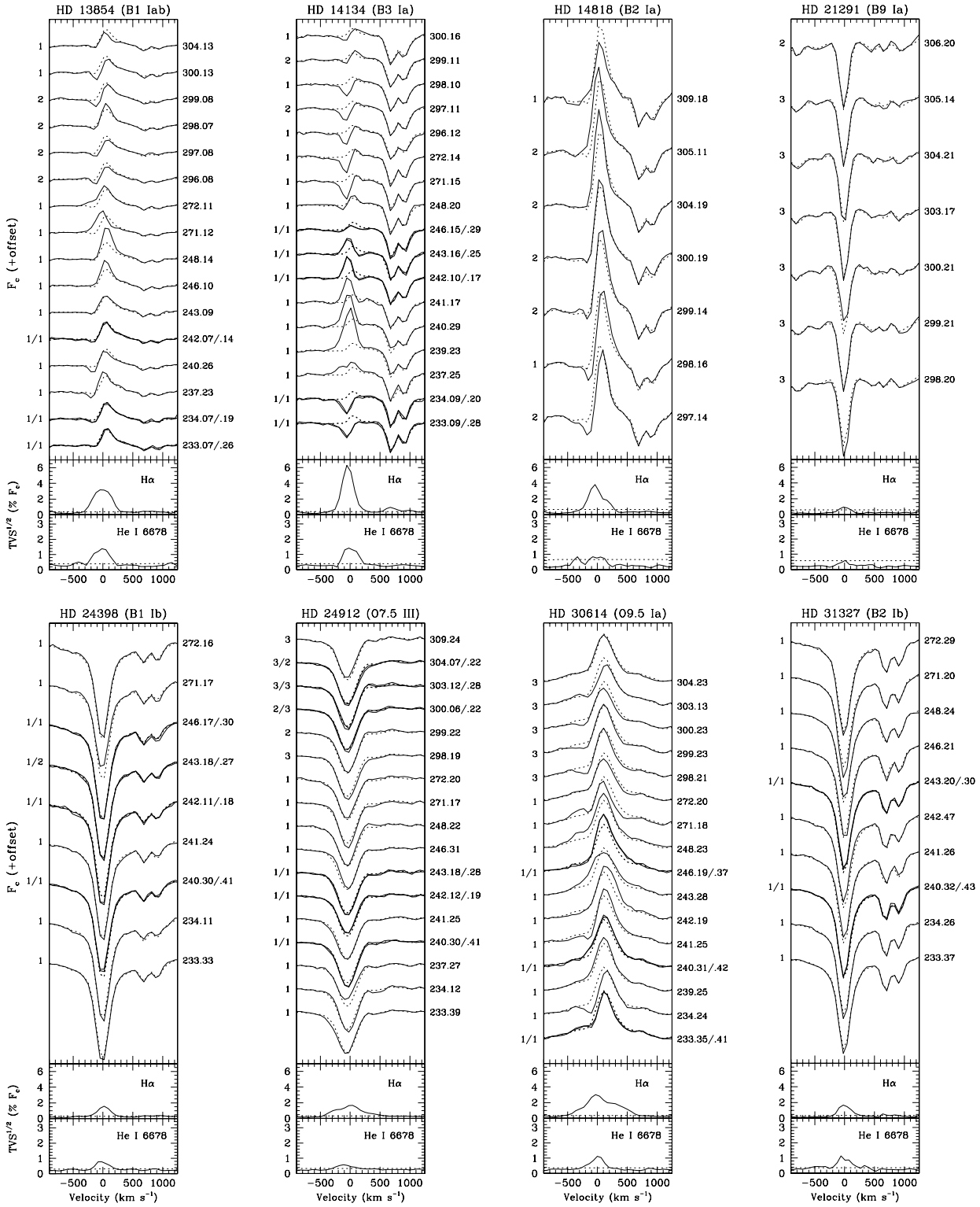

Figure 1. Hα time series for HD 13854, HD 14134, HD 14818, HD 21291, HD 24398, HD 24912, HD 30614 and HD 31327. The spectra are displayed in the stellar rest frame. Consecutive spectra are shifted by 0.15, 0.10, 0.10, 0.07, 0.10, 0.10, 0.10 and 0.10 continuum units, respectively. The mean profile is overplotted as a dashed line. The numbers to the left-hand and right-hand sides of the upper panels give the number of consecutive exposures used to form the corresponding spectrum and the mean Julian date of the observations (HJD – 2 452 000), respectively. The two bottom portions of each panel show the TVS of Hα and He I λ6678 (Fullerton et al. 1996), along with the threshold for a significant variability at the 99.0 per cent confidence level (dashed line). The rest of Fig. 1, displayed over the following pages, shows the Hα time series for HD 37128, HD 37742, HD 38771, HD 41117, HD 42087, HD 43384, HD 47240 and HD 52382 (consecutive spectra are shifted by 0.12, 0.13, 0.08, 0.20, 0.10, 0.12, 0.15 and 0.10 continuum units, respectively), the Hα time series for HD 53138, HD 58350, HD 91316 and HD 119608 (consecutive spectra are shifted by 0.10 continuum units in all cases), and the Hα time series for HD 151804 and HD 152236 (consecutive spectra are shifted by 0.20 and 0.40 continuum units, respectively).

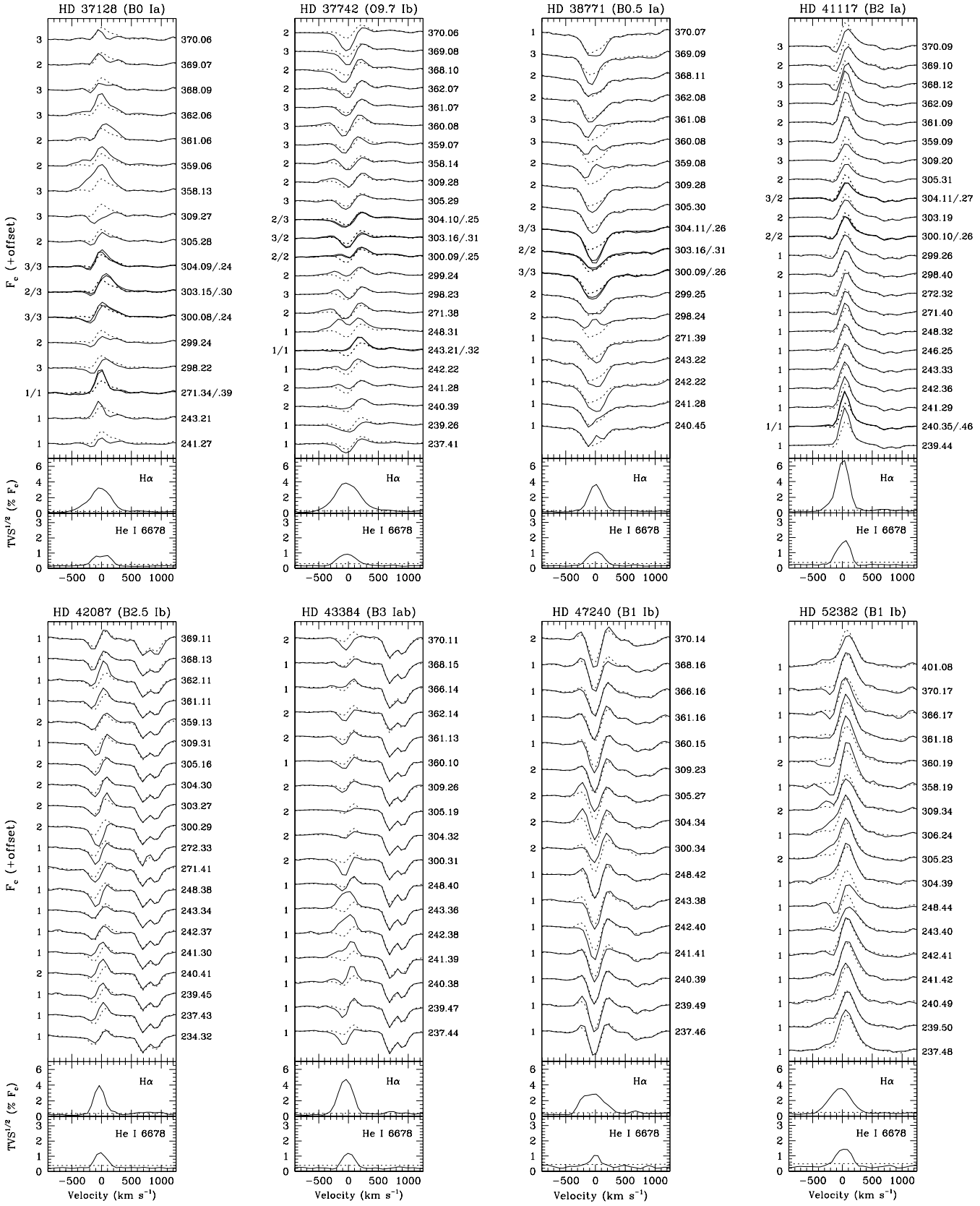

Figure 1 – *continued*

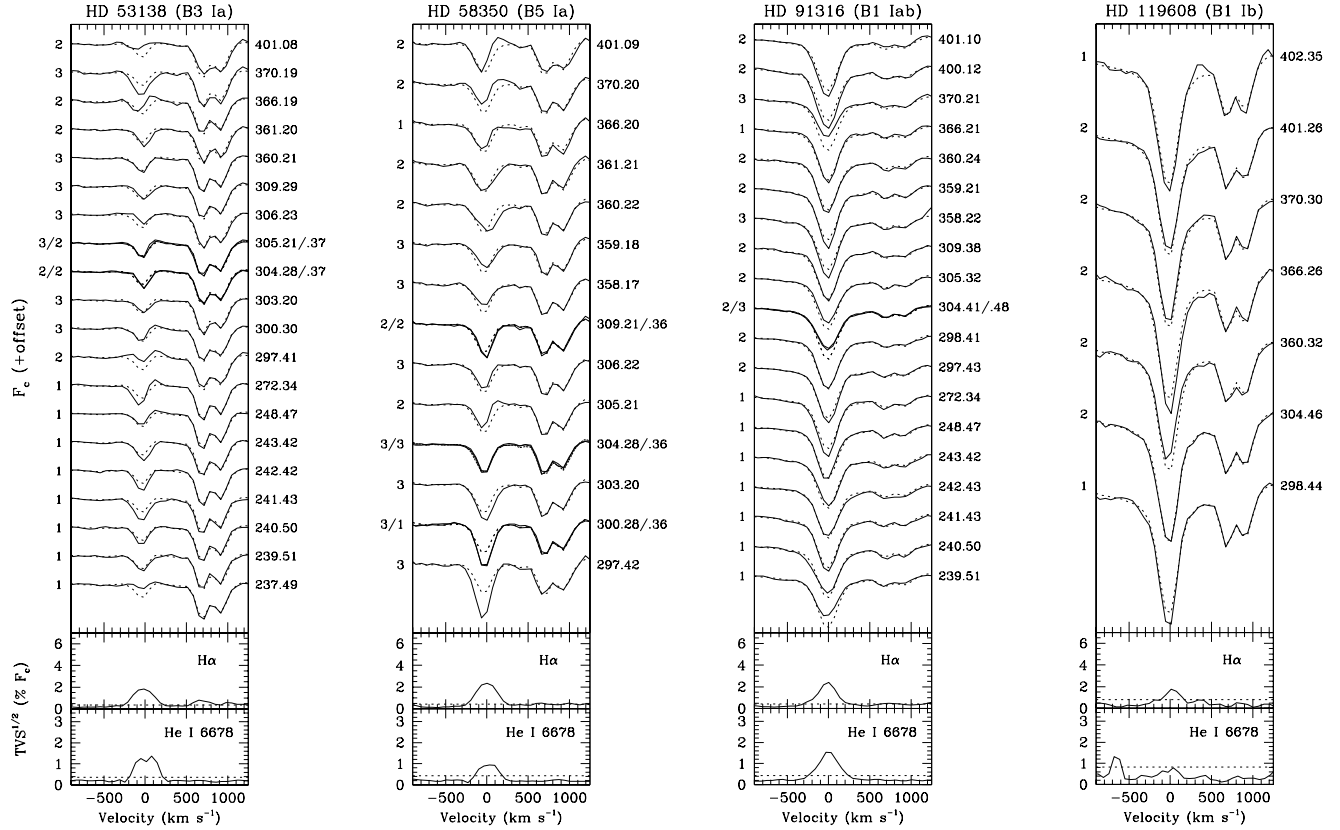

Figure 1 – *continued*

5.1 Photometric data set

Periodicities in the range 1–27 d have been found for nine stars in our sample. Several stars display significant variability at the 0.03–0.07 mag level without, however, evidence for cyclical changes. A complex, multiperiodic behaviour cannot be ruled out in this case. As can be seen in Fig. 2, our photometric observations of HD 13854, HD 14134, HD 14818 and HD 47240 support the periodic nature of the variations suggested by the *Hipparcos* data. This demonstrates the remarkable long-term (years) coherency in the patterns of variability; folded with the appropriate periods, practically all the new data points stay well within the scatter limits (mainly intrinsic, considering the typical accuracy of the *Hipparcos* photometry), *without* any adjustment of the initially chosen zero phases.

5.2 Spectroscopic data set

The significance of the peaks in the PS can be, in principle, rigorously estimated after normalization by the variance of the data (e.g. Scargle 1982). In the case of unevenly spaced time series, however, the false alarm probability (FAP) is only indicative and cannot be used as a robust indicator of the presence of periodic signals in the data (see, for example, Antokhin et al. 1995). While assessing the reality of the periods found in our spectroscopic data set, we therefore took into account additional criteria. Namely, we inspected the period-folded EW/line-profile data, and compared the EW and two-dimensional (2D) pixel-to-pixel PS (even though the line-profile variations are obviously not necessarily accompanied by significant EW changes). The existence of a cyclical pattern of variability is suggested for nine stars out of the 17 included in the analysis. These

Table 4. Photometric and spectroscopic activity indices.

Name	$a_{\rm phot}$		$a_{\rm lpv}$	
	This study (mmag)	*Hipparcos* (mmag)	Hα (per cent)	He I λ6678 (per cent)
HD 13854	26	13	47.3	10.6
HD 14134 (V520 Per)	22	24	259	11.2
HD 14818 (10 Per)	20	17	34.8	6.01
HD 21291		17	12.5	0[b]
HD 24398 (ζ Per)		0	5.91	5.57
HD 24912 (ξ Per)		0	14.6	6.53
HD 30614 (α Cam)		9	17.8	10.7
HD 31327		0	6.45	7.92
HD 37128 (ϵ Ori)		11	81.9	7.66
HD 37742 (ζ Ori A)		4	82.7	11.0
HD 38771 (κ Ori)		9	32.6	7.35
HD 41117 (χ^2 Ori)		15	27.9	12.8
HD 42087 (3 Gem)	20:	13	91.2	8.98
HD 43384 (9 Gem)		20	135	7.69
HD 47240	17	5	40.2	5.89
HD 52382	20	16	32.1	11.0
HD 53138 (o^2 CMa)		21	66.4	9.64
HD 58350 (η CMa)		28	44.1	6.90
HD 91316 (ρ Leo)		9	12.8	10.1
HD 119608		0	10.2	0[b]
HD 151804		0[a]	5.16	0[b]
HD 152236 (ζ^1 Sco)		22	5.66	19.1

[a]Photometric variable according to Balona (1992), and references therein.
[b]These stars do not exhibit significant variability in He I λ6678 (see Fig. 1).

cases are individually discussed below. No indication of a cyclical behaviour was found in HD 24398, HD 30614, HD 31327, HD 43384, HD 52382, HD 53138, HD 58350 and HD 91316. Kaper et al. (1998) and Markova (2002) report variations on a time-scale of about one week in HD 30614. A search for periodic modulations of the UV lines in HD 53138 proved inconclusive, in line with our non-detection (Prinja et al. 2002).

HD 13854: significant power at $\nu \sim 0.955$ d^{-1} is found in the EW data (Fig. 3), but not in the Hα time series.

HD 14134: this star does not exhibit any evidence for binarity (Abt & Levy 1973). The photometric variability of HD 14134 is relatively well documented (Rufener & Rufener 1982; Waelkens et al. 1990; Krzesiński, Pigulski & Kołaczkowski 1999; Adelman, Yüce & Engin 2000), but the *Hipparcos* data provide the first clear evidence for a periodic pattern with $\mathcal{P} \sim 12.823$ d (Fig. 2). Two periodic signals at $\nu_1 = 0.045$ and $\nu_2 = 0.080$ d^{-1} ($\mathcal{P} \sim 22.2$ and 12.5 d, respectively) are unambiguously detected in the 2D PS, with FAP $\lesssim 0.1$ per cent (see Fig. 4). The latter frequency is also found in the EW PS (once again with FAP $\lesssim 0.1$ per cent) and is, within the errors, identical to the value found in the photometric data. The non-detection of ν_1 both in the EW and in the photometric data sets leads us to take ν_2 as the fundamental frequency. The two signals are likely to be simple harmonics ($\nu_2 \sim 2\nu_1$). As can be seen in Fig. 5, maximum Hα emission nearly coincides with maximum light. We use the photometric ephemeris when folding the EWs ($\mathcal{P} = 12.823$ d and $T_0 = 2\,447\,867.8$), as this period is indistinguishable, but more accurate, than the value derived from the spectroscopic data.

The clearly phase-locked nature of the variations is reminiscent of some early-type stars displaying evidence for a decentred, dipole magnetic field (e.g. Stahl et al. 1996). A single circular polarization spectrum of HD 14134 was therefore obtained on 2003 July 29 using the MuSiCoS spectropolarimeter at the 2-m Bernard Lyot telescope

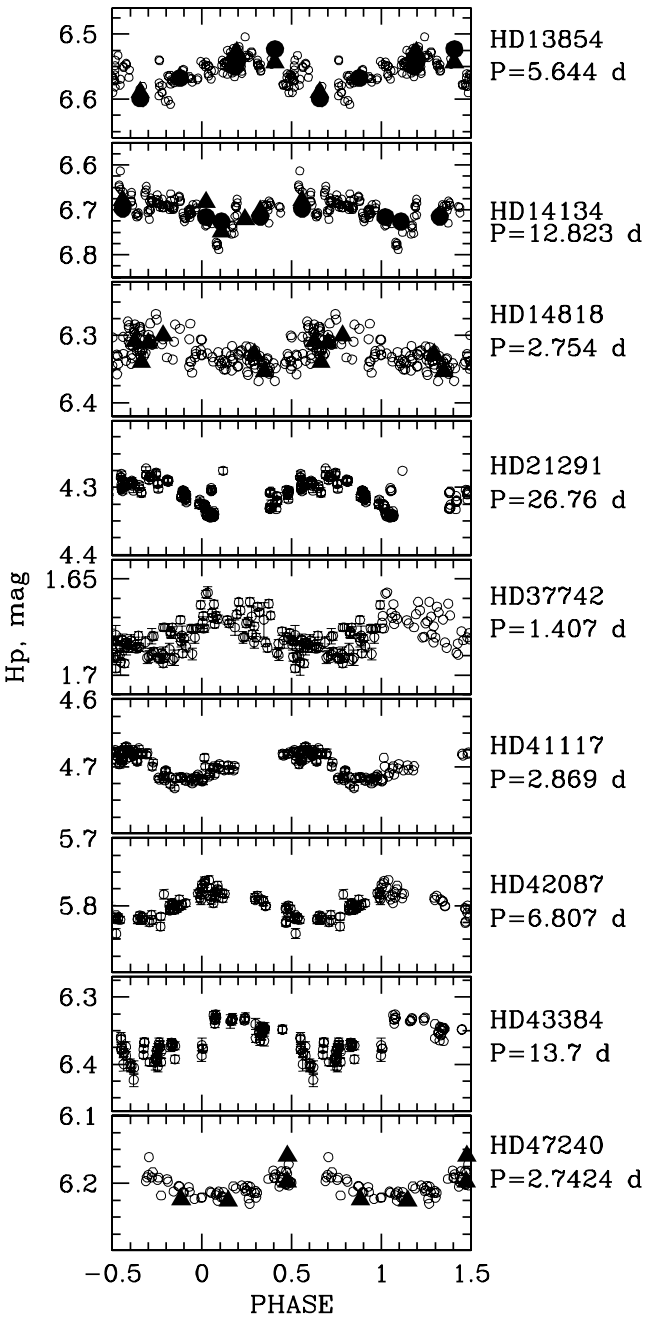

Figure 2. *Hipparcos* light curves for stars displaying periodic variations. Zero phase is arbitrarily assigned to the start of the observations. The size of the symbols approximately corresponds to 2-σ error bars (if not shown). Our *B*- and *I*-band observations are overplotted as filled triangles and circles, respectively (the points are vertically shifted by a constant value to match the *Hipparcos* data). In this case the size of the symbols corresponds to 4-σ error bars.

(Pic du Midi Observatory). The peak S/N ratio was 250 (weather conditions were relatively poor). The mean profiles obtained using the least-squares deconvolution (LSD) procedure (Donati et al. 1997) show no significant circular polarization within spectral lines. The measured longitudinal magnetic field is 45 ± 145 G (G. A. Wade, private communication).

HD 24912: de Jong et al. (1999) discussed periodic changes in photospheric lines that may arise from pulsations ($\mathcal{P} \sim 3.45$ h).

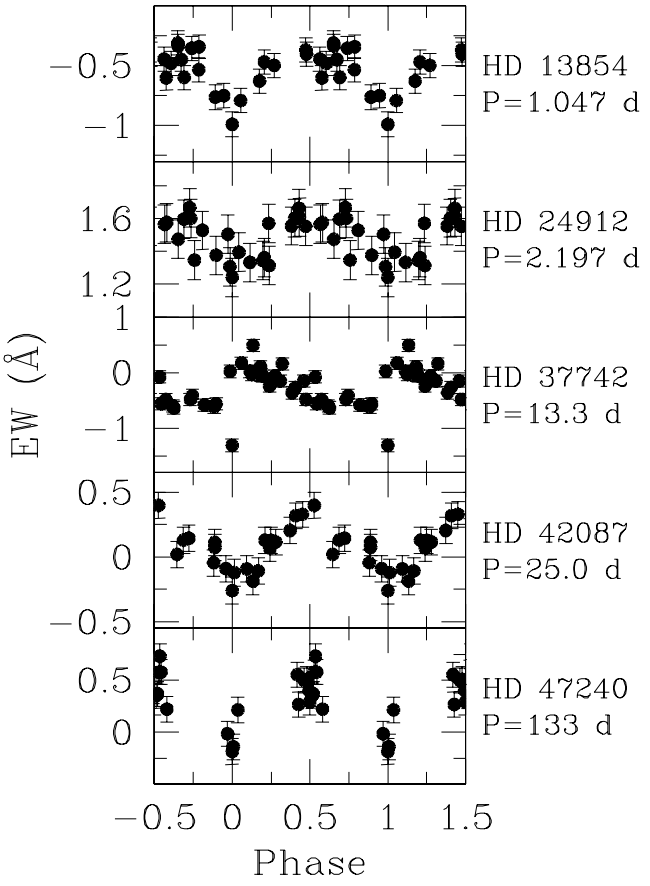

Figure 3. EW of the Hα line as a function of phase (data for HD 14134 in Fig. 5). Zero phase is arbitrarily set at maximum emission (or, alternatively, at minimum absorption). The uncertainties have been calculated following Chalabaev & Maillard (1983).

This star presents a strong case for a persistent, cyclical variability in the UV wind line profiles with $\mathcal{P} \sim 2$ d (Kaper et al. 1997). From an analysis of an extensive data set of UV and optical observations, de Jong et al. (2001) reported a 2.086-d modulation of the line profiles, notably in Hα. In our data we find indication for a period tantalizingly close to, but apparently significantly different from this value: $\mathcal{P} \sim 2.20$ d (with a typical uncertainty of 0.03 d). There is also some evidence for long-term changes in the pattern of variability. While cyclical variations are suggested here in the red wing of Hα (Fig. 4), such changes predominantly occurred in the blue wing in 1994 October (de Jong et al. 2001). Although the periodic signal found in our data is present both in the Hα line profile and EW time series, we warn that its formal significance is low in the 2D PS (Fig. 4), while the phase-locked nature of the EW variations is only marginal (Fig. 3).

HD 37128: Prinja et al. (2002) discussed the UV line-profile variations in this star, but the limited time-span of the *IUE* observations ($\sim$17 h) precluded the detection of a cyclical behaviour on a rotational time-scale. Three signals are detected at the 99.0 per cent confidence level in the pixel-to-pixel Hα PS at $\nu_1 = 0.055$, $\nu_2 = 1.070$ and $\nu_3 = 1.280$ d^{-1} (Fig. 4). ν_2 can be identified as the 1-d alias of ν_1. Interestingly, the highest peaks in the EW PS correspond to the two remaining signals, although with low significance level, as confirmed by the poorly coherent patterns of variability. Our data therefore suggest the existence of two periods at $\mathcal{P} \sim 18.2$ and 0.78 d, but at a low confidence level.

HD 37742: line-profile variations on a time-scale of about 6 d are suggested both in Hα and in UV wind lines (Kaper et al. 1998, 1999). Several significant peaks (all with FAP $\lesssim 1$ per cent) are found in the pixel-to-pixel PS at $\nu_1 = 5 \times 10^{-3}$, $\nu_2 = 0.020$, $\nu_3 = 0.880$ and $\nu_4 = 1.148$ d^{-1} (Fig. 4). Only ν_4 is found in the EW data set, but this signal is likely spurious, as judged from the lack of coherent variations. Alternatively, the EW variations appear reasonably phase-locked when folded with $\nu_5 = 0.075$ d^{-1} (Fig. 3). This signal is also found in the pixel-to-pixel PS, but the confidence level is low.

HD 38771: two signals are found in the 2D PS (see Fig. 4) at $\nu_1 = 0.210$ (FAP ~ 5 per cent) and $\nu_2 = 0.955$ d^{-1} (FAP ~ 1 per cent), but there is no evidence for periodicity in the EW time series.

HD 41117: several peaks are found in the 2D PS (all with FAP $\lesssim 1$ per cent) at $\nu_1 = 5 \times 10^{-3}$, $\nu_2 = 0.025$ (and its first harmonic at 0.050 d^{-1}), $\nu_3 = 1.045$ and $\nu_4 = 1.085$ d^{-1} (Fig. 4). The highest peaks in the EW PS are found at $\nu_5 = 0.025$, $\nu_6 = 0.065$ and $\nu_7 = 0.205$ d^{-1}. Among these, ν_6 and ν_7 can be ruled out from the lack of phase-locked EW variations. Despite the detection of ν_5 both in the 2D and in the EW PS, the poorly coherent pattern of variability casts serious doubt on the existence of this 40-d signal.

HD 42087: this star does not exhibit significant radial velocity variations (Mayer et al. 1998). The highest peak in the 2D PS is found at $\nu_1 = 0.040$ d^{-1}, and appears both in the emission component and in the absorption trough of the Hα P Cygni profile (Fig. 4). Although its formal significance is relatively low (FAP ~ 5 per cent), the existence of a 25-d periodicity is supported by the EW data (Fig. 3).

HD 47240: there is a tentative indication that the changes in Si IV λ1400 are repetitive over a 3–5 d time-scale (Prinja et al. 2002). An ill-defined, long-term periodic signal is found in the EW data set at $\nu_1 = 0.0075$ d^{-1}, along with smaller peaks at $\nu_2 = 0.105$ and $\nu_3 = 0.247$ d^{-1}. The two latter frequencies are likely spurious, as judged from the poorly coherent nature of the phased EW variations. Interestingly, ν_1 is also found in the pixel-to-pixel Hα PS with a confidence level close to 95 per cent (Fig. 4). However, both the close correspondence with the total time-span of the observations (see Table 3) and the sparsely sampled EW data (Fig. 3) lead us to discard it from further consideration. Furthermore, the Hα morphology is typical of a fast-rotating star seen nearly equator-on (Conti & Leep 1974; Petrenz & Puls 1996). It is therefore unlikely that spectral changes operating on such a long time-scale would be associated with rotation. Variations intrinsic to a circumstellar disc-like enhancement cannot be ruled out a priori, but they would manifest themselves as V/R variations of the line emission peaks, which are not observed (Fig. 4).

6 DISCUSSION

6.1 Incidence of cyclical line-profile variations

The results of our period search are summarized in Table 2. Several of the listed periods must be regarded as tentative, especially those detected either in the 2D or in the EW PS. Independent confirmation is clearly needed in this case. We also recall that HD 13854 and HD 47240 might be part of a close, massive binary system (Section 3.1). Because our survey was not designed to detect short-term periodicities, the found periods close to 1 d must also be regarded with some caution. They might arise from rotational modulation only for the fastest rotators. Conversely, they might be associated with the pseudo-periodic ejection of 'puffs' of material. Such an outward propagation of density perturbations has been proposed to account for the recurrent changes (with a time-scale of $\sim$20 d) in the Hα line of the B0.5 hypergiant HD 152236 (Rivinius et al.

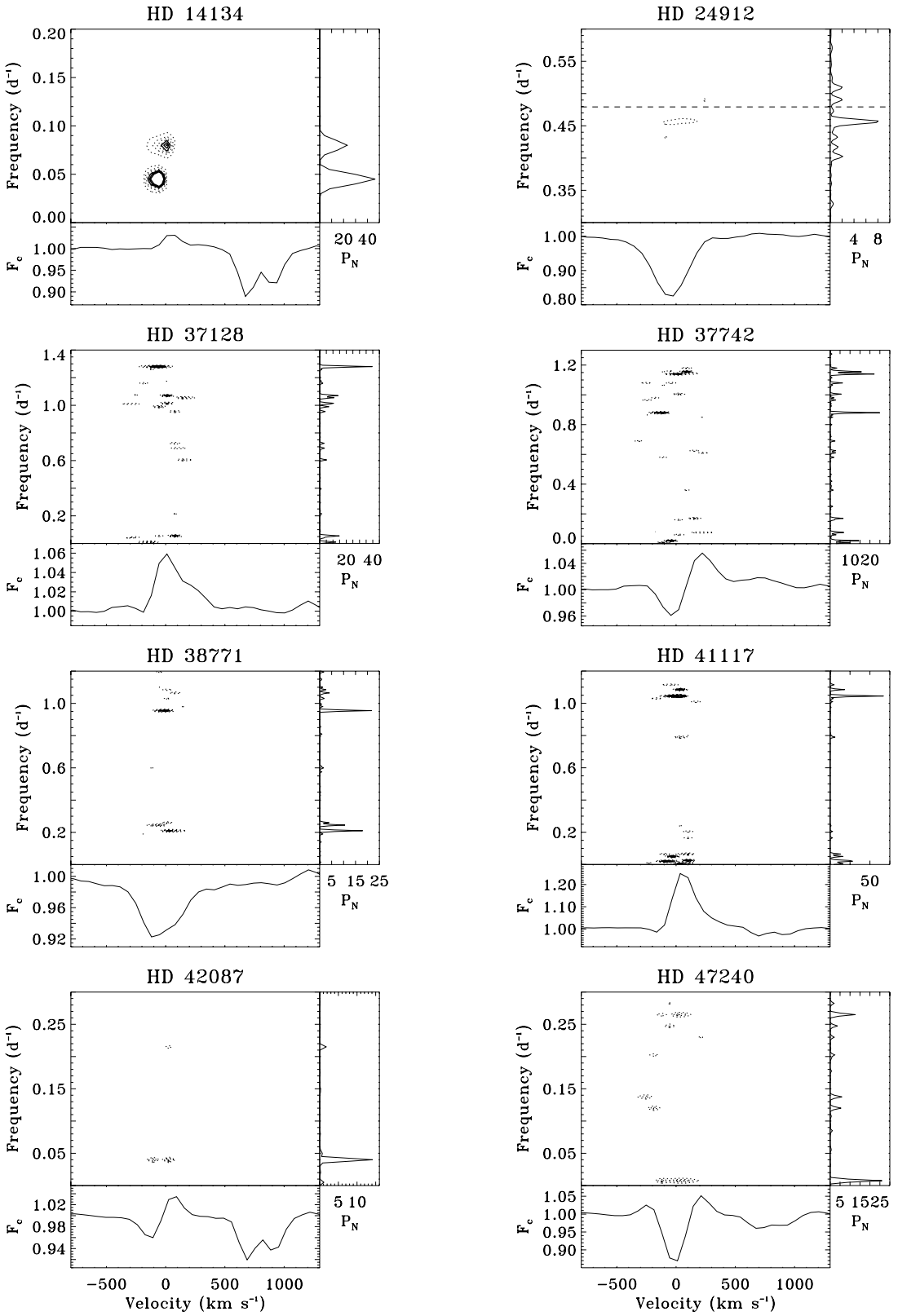

Figure 4. Pixel-to-pixel PS of the Hα time series. The number of iterations and gain of the CLEAN algorithm were typically set to 2000 and 0.6, respectively. All the PS are variance-normalized to provide a uniform assessment of significance. The solid contours are drawn for intensities of 12.9, 10.6 and 8.0 (this corresponds to significance levels of 99.9, 99.0 and 95.0 per cent, respectively). The dotted contours are drawn for intensities of 7.0, 5.0, 3.0 and 1.0. In each diagram, the frequency range is chosen to show more clearly the detected signals; no significant power peaks are found outside this frequency domain. For HD 24912, the dashed line indicates the 2.086-d period found by de Jong et al. (2001). The bottom section of each panel shows the mean spectrum (in the stellar rest frame), while the side panel presents the PS summed over the shown velocity range.

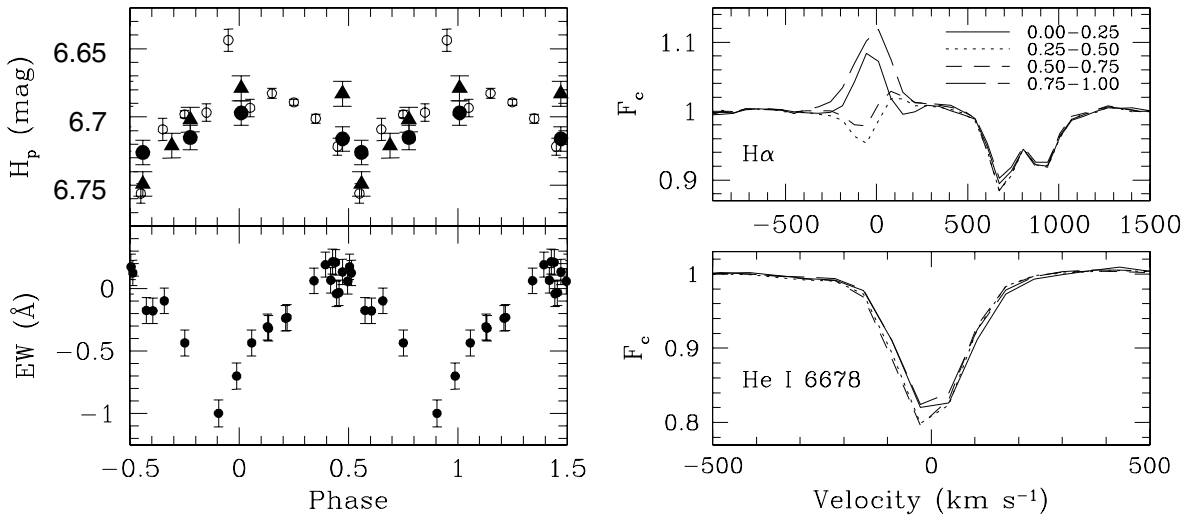

Figure 5. Left-hand panels: light curve of HD 14134 binned to 0.1 phase resolution (symbols as in Fig. 2; here note that zero phase is arbitrarily set at maximum light) and EWs of the Hα line, as a function of phase. Right-hand panels: phase-averaged Hα and He I λ6678 profiles. In all cases we use the photometric ephemeris: $P = 12.823$ d and $T_0 = 2\,447\,867.8$.

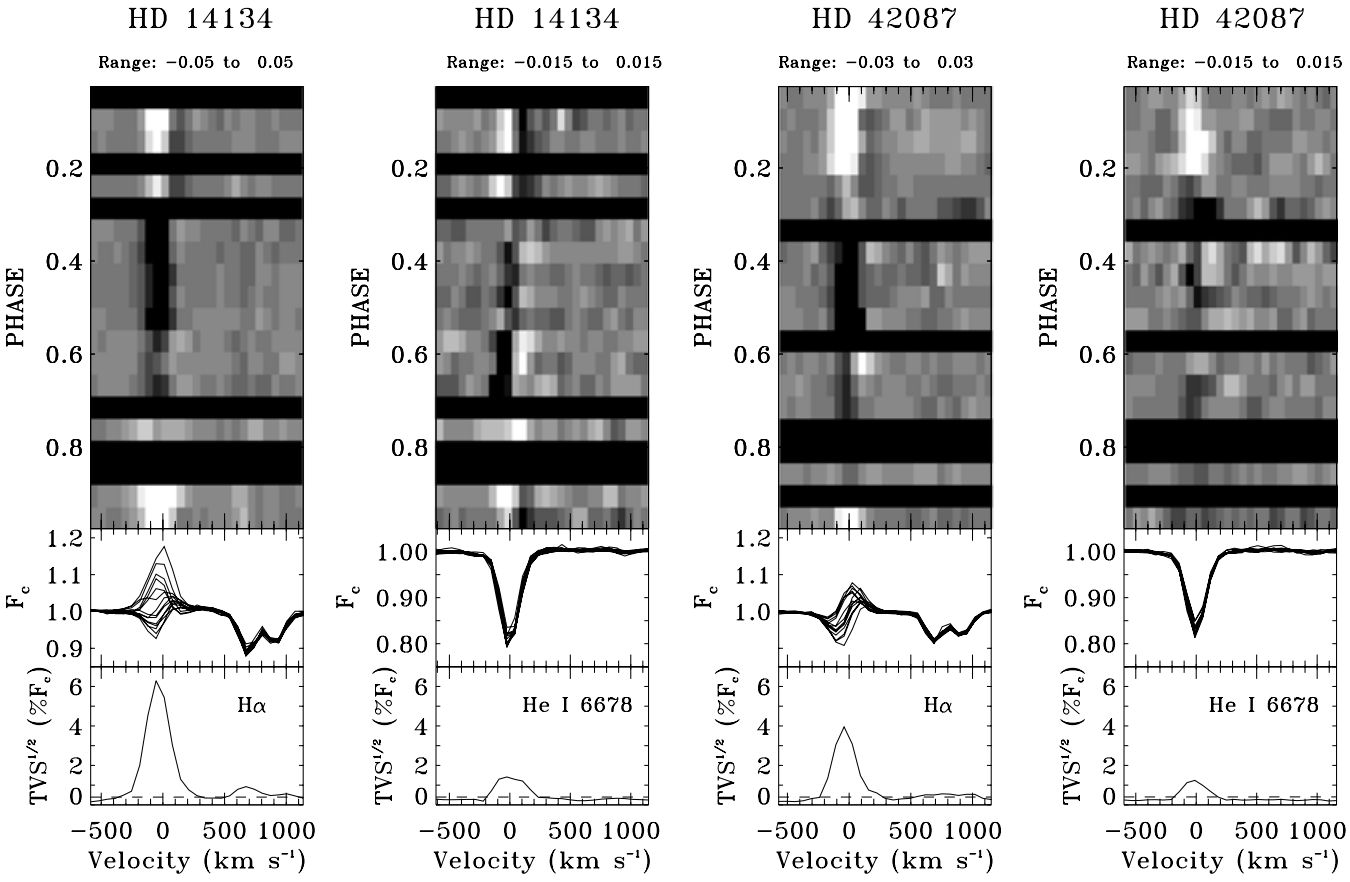

Figure 6. Grey-scale plots of the residuals of Hα and He I λ6678, as a function of phase, for HD 14134 ($P = 12.823$ d) and HD 42087 ($P = 25.0$ d). The residual profiles are the individual spectra binned to 0.05 phase resolution minus the mean spectrum. Excess emission (or, alternatively, weakening of absorption) appears brighter in these plots. We use the photometric ephemeris in the case of HD 14134, while zero phase is arbitrarily fixed at maximum emission for HD 42087. The middle portion of each panel shows the superposition of the binned profiles. The TVS, along with the horizontal dashed line indicating the 99.0 per cent confidence level for significant variability, are displayed in the lower portion of each panel. The grey-scale plots are displayed in the stellar rest frame.

1997). Changes on a time-scale of about 1 d might be compatible with the characteristic flow time through the Hα line-formation region in our programme stars, provided that these putative, spatially-localized density enhancements follow a β-type velocity law with an exponent close to unity.[3] Although such an interpretation cannot be completely ruled out, it should be noted that HD 152236 is considered as a candidate luminous blue variable and is likely not representative of the stars in our sample (Sterken, de Groot & van Genderen 1997). Pulsations can also operate on a 1-d time-scale, but we find no trivial relation between the spectroscopic and photometric periods (the latter presumably related to pulsations, as argued below).

Summarizing, we consider that the two stars with a relatively long-term periodic modulation seen both in the EW and in the line-profile data sets present the strongest cases for a cyclical behaviour: HD 14134 and HD 42087 (with $\mathcal{P} \sim 12.8$ and 25.0 d, respectively). The phase-related patterns of variability are remarkably similar (see Fig. 6). In addition, the line-profile changes in Hα and He I λ6678 also seem to be correlated in both stars, with excess emission in Hα being accompanied by a weakening of He I λ6678. As can be seen in Fig. 5, this may also apply to weak metal lines such as C II λ6578.05 and C II λ6582.88 (note that variations in the continuum level may be invoked in the case of HD 14134 in view of the large, phase-locked photometric variations). Because a significant amount of incipient wind emission is not expected for stars with such relatively low mass-loss rates (Table 1), this phenomenon may point to a link between the wind variability and photospheric disturbances. Higher-resolution data are, however, needed to reveal an organized pattern of variability in photospheric lines, as observed in other B-type supergiants (Kaufer et al. 1997, 2002).

The lack of cyclical variations for several stars in our sample can have a physical origin or may be ascribed to the limitations of the current data set (e.g. insufficient time sampling). The large amplitude of the variations exhibited by most stars suggests that an imperfect removal of telluric features or S/N issues are probably irrelevant. We may be more concerned by the fact that our observations were relatively few and spread out over several months. If we accept the idea that large-scale wind streams give rise to the variability, substantial variations in the global wind morphology might be expected on a time-scale of months/years (as in the case of the B0.5 Ib star HD 64760; Fullerton et al. 1997). A lack of coherency in the pattern of variability on a monthly time-scale would thus not be surprising, especially for the fastest rotators in our sample. It is unlikely in this case that a strong periodic signal would appear in the data. Another issue which may lead to a loss of periodic signal is the complex pattern of variability presented by Hα in B supergiants (see, for example, Kaufer et al. 1996; de Jong et al. 2001; Prinja et al. 2001), emphasizing the need for high spectral/time resolution.

6.2 Evidence for rotational modulation?

Detailed studies of the line-profile variations in the UV domain have inferred a rather simple geometrical structure for the wind of some B supergiants, with generally two (or four) symmetrical, spatially-extended wind streams (e.g. Fullerton et al. 1997). Consequently, one generally expects the recurrence time-scale of the line-profile variations to be an integer fraction of the stellar rotational period, rather than the period itself. In HD 24912, for instance, the period found in Hα can be identified, within the uncertainties, with one half of the rotation period (de Jong et al. 2001). The fact that the periodicity found in the spectroscopic data set for HD 42087 is longer than the estimated maximum rotational period is therefore puzzling in this respect (Table 2). Apart from rotation, however, there is a clear indication for the existence of an additional (perhaps dominating) line broadening mechanism in B-type supergiants (plausibly tangential macroturbulence; Howarth 2004). The projected rotational velocities are thus likely to be grossly overestimated for the stars in our sample, with the result that the true rotational periods may be significantly longer than anticipated (Ryans et al. 2002). The modulation time-scale of Hα in HD 14134 and HD 42087 is commensurate with the probable rotation periods, but rotational modulation cannot be firmly established in view of these uncertainties. For the former, the 12.8-d period found is close to the estimate of the minimum rotational period ($\sim$10 d), which would imply that this star is a fast rotator viewed almost equator-on. However, because in HD 14134 the $v \sin i$ is typical of stars of the same spectral type (Howarth et al. 1997), this 12.8-d time-scale is more likely to be an integer fraction of the rotation period.

The prominent changes affecting the P Cygni absorption component of the Hα line in HD 14134 and HD 42087 (Fig. 6) may diagnose variations in the amount of wind material seen projected against the stellar disc because of an azimuthal dependence of the mass-loss rate. Note in this respect that in HD 14134 maximum Hα emission and maximum light do not seem to exactly coincide (see Fig. 5). The existence of such a phase offset (which needs to be confirmed thanks to a more accurate ephemeris) would be consistent with a picture in which photospheric perturbations lead to the development of large-scale, spiral-shaped wind structures (Cranmer & Owocki 1996). Let us suppose a bright photospheric region causing a local enhancement of the mass-loss rate. We observe a classical P Cygni profile when this 'overloaded' portion of the wind is projected against the stellar disc. However, the motion of this wind feature towards the stellar limb because of rotation will cause the growth of Hα emission. A small phase lag (i.e. $\Delta\phi < 0.25$) would be expected if the spot has significant azimuthal extent. A substantial modulation of the local mass-loss rate may also be invoked to explain the large, phase-locked EWs variations seen in other stars (e.g. HD 13854; Fig. 3).

6.3 Relation to photospheric variability

The hypothesis that the development of azimuthally structured outflows in early-type stars is intimately linked to processes taking place at the photosphere (Cranmer & Owocki 1996) has received considerable observational support (e.g. Henrichs, Kaper & Nichols 1994; Reid & Howarth 1996). Much more controversial, however, is the nature of the 'seed' perturbations, with pulsational and magnetic activity as the most straightforward candidates. In the light of our results, we discuss below the relevance of these two scenarios in B-type supergiants.

6.3.1 Pulsations

The *Hipparcos* data have revealed the existence of a large population of B-type supergiants with daily, quasi-periodic light variations. These stars might constitute the extension to higher luminosities of

[3] Here we do not consider the outward propagation of small-scale clumps of material resulting from the unstable nature of radiatively-driven winds, as this would lead to a *stochastic* pattern of variability (e.g. Eversberg, Lépine & Moffat 1998).

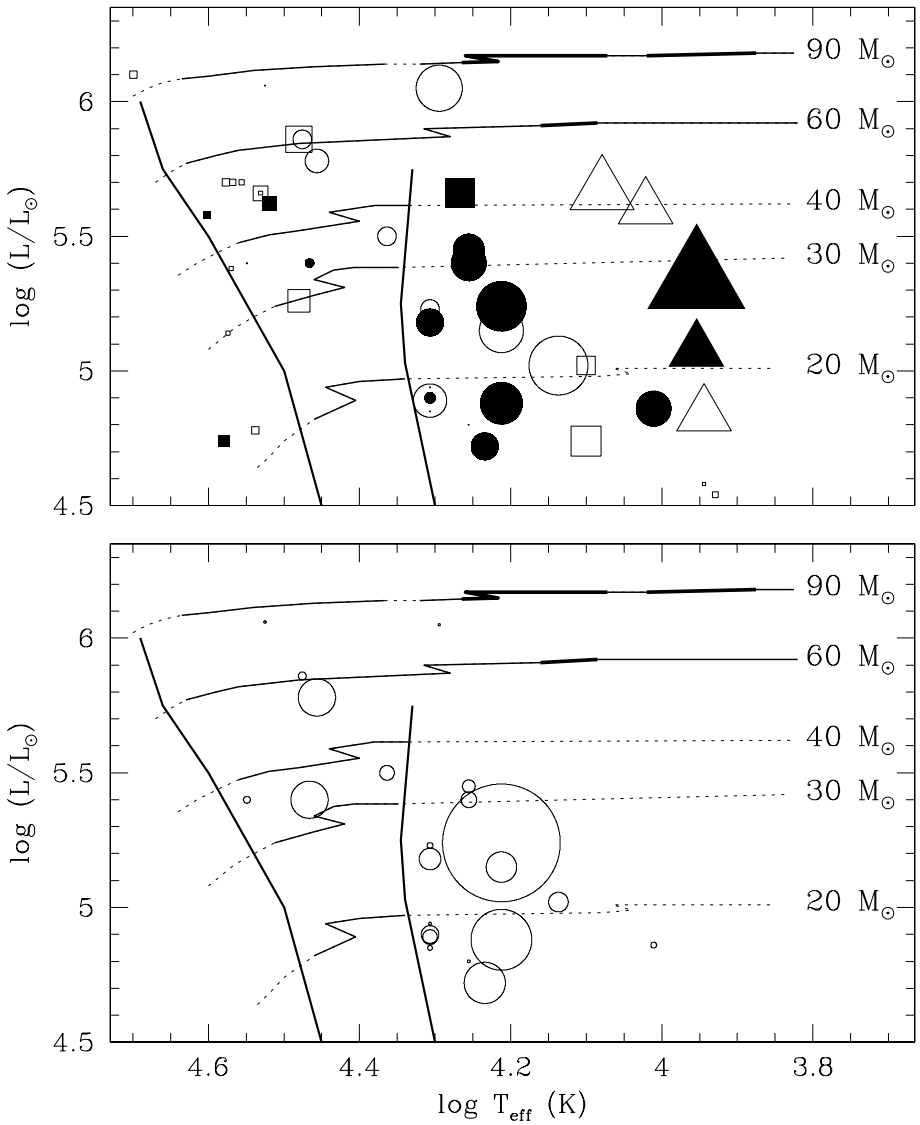

Figure 7. Upper panel: the circles show the positions of the programme stars in the HR diagram (some stars have been slightly shifted along the ordinate axis for the sake of clarity). The size of the symbols is directly proportional to the amplitude of the photometric variations in the *Hipparcos* data, $a_{\rm phot}$ (see Table 4). The squares and triangles show the position of galactic OBA-type stars (van Genderen et al. 1989) and blue supergiants in NGC 300 (Bresolin et al. 2004), respectively. The size of the symbols is proportional in this case to the amplitude of the variations in the *V* band. Filled and open symbols correspond to stars with and without evidence for photometric periodicities, respectively. Lower panel: positions of the programme stars in the HR diagram with the size of the symbols being proportional to the fractional amplitude of the line-profile variations in Hα, $a_{\rm lpv}$. The evolutionary tracks (dotted lines) have been calculated for solar metallicity and for the various initial masses indicated to the right-hand side of the panels. Domains of the strange mode oscillations are overplotted as solid lines, while thick lines correspond to very unstable phases (from Kiriakidis et al. 1993). The pulsational instability strip of non-radial g-type modes is shown as (nearly vertical) solid lines. The models have been calculated using the OPAL opacities, a hydrogen abundance, $X = 0.70$, and a heavy element abundance, $Z = 0.02$ (from Pamyatnykh 1999).

the slowly pulsating B stars, suggesting the κ-mechanism excitation of multiple, non-radial gravity modes arising from a metal opacity bump at $T \sim 2 \times 10^5$ K in stellar interiors (e.g. Waelkens et al. 1998). Both the amplitude and the time-scale of the photometric variations are compatible to what is observed in our sample. To investigate this issue in more detail, we plot in Fig. 7 our stars on a Hertzsprung–Russell (HR) diagram, along with the theoretical instability strips for non-radial g modes calculated without mass loss and rotation (Pamyatnykh 1999). The stars with a clear cyclical behaviour (a sample evidently biased towards the stars with large photometric amplitudes) do not appear to fall in the predicted domains of pulsational instability. The non-local thermodynamic equilibrium (NLTE) spectral synthesis of Kudritzki et al. (1999) suggests systematically higher effective temperatures and luminosities for some stars included in our study. However, such a temperature offset may not be sufficient to bring these stars in the instability zone. Furthermore, only the late B-type stars in our sample seem to follow the period–luminosity relation for g modes (see fig. 3 of Waelkens et al. 1998). Massive stars are also believed to experience a variety of strange-mode and resonance instabilities (Kiriakidis, Fricke & Glatzel 1993), but there is no indication that the photometric variations are related to this phenomenon (Fig. 7). The ubiquity of pulsational instability in this part of the HR diagram (e.g. Fullerton et al. 1996; Kaufer et al. 1997) leads us to consider pulsations as

most likely responsible for the photometric variations, although it is clear from the above discussion that the pulsation modes have yet to be identified in this case. The apparent dichotomy between the photometric properties of O and B supergiants seen in Fig. 7 (the former exhibiting significantly lower variability amplitudes) suggests that the pulsations are of different nature in these two classes of objects (e.g. higher modes are excited in O-type stars).

The complete absence of the photometric periods in the Hα time series (HD 14134 excluded) seems at first glance to argue against pulsations as driver of the wind variability (once again under the assumption that the light variations can be ascribed to this mechanism). As can be seen in Fig. 7, the stars displaying the highest level of Hα variability are not preferentially found close to the zones of pulsational instability. This hypothesis can be investigated further by looking for a correlation between the amplitude of the photometric and Hα changes, as parametrized by the activity indices $a_{\rm lpv}$ and $a_{\rm phot}$ (the latter calculated from *Hipparcos* data; Section 4). Although there is a hint of a positive correlation (FAP $\sim$ 2.3 per cent), this trend disappears when the four stars displaying line-profile variations that cannot be unambiguously related to wind activity, but can be of purely photospheric origin, are excluded (i.e. HD 21291, HD 24398, HD 31327 and HD 119608). In addition, there is also no correlation between $a_{\rm lpv}$ (Hα) and $a_{\rm lpv}$ (He I λ6678).

The lack of a clear statistical relationship between the levels of activity at the photosphere and at the base of the outflow (as diagnosed by the photometric changes/He I λ6678 and Hα, respectively) suggests that the same physical mechanism (i.e. presumably pulsations) is not responsible for the photospheric and wind activity. This conclusion relies, however, on statistical grounds and should be in principle examined on a star-to-star basis; here, we note the example of HD 64760, where the same periodic signal seems to appear in photospheric and wind lines (Kaufer et al. 2002). Although detailed models are still lacking, we may also expect a complex interplay between any pulsation signal and wind changes (e.g. beating of some pulsation modes). This is likely to result in a loose (if any) relationship between photometric and Hα changes, for instance.

6.3.2 Magnetic fields

A growing amount of evidence suggests the existence of weak magnetic fields in early-type stars, although firm detections are still scarce and might be restricted to some atypical cases. Spectropolarimetric observations of the very young O4–6 star θ^1 Orionis C have revealed a relatively strong magnetic field, 1.1 $\pm$ 0.1 kG (Donati et al. 2002). The existence of a weaker field in the B1 IV star β Cephei (with a polar component of 360 $\pm$ 30 G) has also been reported recently. This field appears to be sufficient to control the outflow at large distances from the star (out to $\sim 9R_\star$; Donati et al. 2001). Magnetic activity in OB stars is also hinted at by X-ray observations of the O9.5 II star HD 36486 (δ Ori) and HD 37742 (Waldron & Cassinelli 2000; Miller et al. 2002), which challenge the generally accepted view that the X-ray emission in early-type stars solely arises from outwardly propagating shocks developing as the result of the inherently unstable nature of radiation-driven winds (see also Feigelson et al. 2002). Recent theoretical studies indicate that a magnetic field of a moderate strength can be produced via dynamo action at the interface between the convective core and the outer radiative envelope, and brought up to the surface on a time-scale typically shorter than the main-sequence lifetime (Charbonneau & MacGregor 2001; MacGregor & Cassinelli 2003).

Apart from our observations of HD 14134 (Section 5.2), HD 24912 is the only star in our sample for which a magnetic field has been searched for via spectropolarimetric observations. A 3-σ upper limit of 210 G in the longitudinal component was derived (de Jong et al. 2001). It is worth noting that this does not set stringent constraints on the potential role played by magnetic activity, as even relatively weak fields ($B \lesssim 100$ G) are suspected to significantly perturb line-driven flows (Owocki 1994). This issue has been recently worked out in more detail by ud-Doula & Owocki (2002) who studied the influence of a large-scale magnetic field with a dipole configuration on the radiatively-driven outflow of an early-type star. They found that the disturbance imposed by the magnetic forces can be parametrized by a confinement parameter, $\eta = B_{\rm eq}^2 R_\star^2 / \dot{M} v_\infty$, where $B_{\rm eq}$ is the equatorial field strength at the stellar surface. The magnetic field appears to significantly impact on the wind morphology and dynamics even for values as low as $\eta = 0.1$, while the emergent flow is channelled along closed magnetic loops for $\eta \gtrsim 1$. For the physical parameters typical of our programme stars (e.g. HD 14134; see Table 1), we obtain $\eta = 1$ for $B_{\rm eq} \sim 70$ G. In this case the Alfvén radius would be about 2 $R_\star$, i.e. comparable to the extent of the Hα line-formation region (ud-Doula & Owocki 2002). This rough estimate shows that magnetic activity cannot be ruled out as driver of the wind activity at this stage. A much stronger field is unlikely in HD 14134, considering our spectropolarimetric observations together with the lack of strong X-ray emission ($L_{\rm X}$[0.2–4.0 keV] $\lesssim$ 33.0 erg s^{-1}; Grillo et al. 1992). Fields of the same magnitude can also be expected in other stars from our sample in view of their relatively low X-ray luminosities (Berghöfer, Schmitt & Cassinelli 1996).

7 CONCLUSION

Our long-term monitoring has confirmed the ubiquity of Hα line-profile variations in OB supergiants. The changes result from the combined effect of a varying amount of incipient wind emission and an intrinsically variable underlying photospheric profile, with the relative contribution of these two phenomena varying from one star to another. As a consequence of the large amplitude of the Hα variations observed, a precise determination of the stellar atmospheric parameters will not be generally possible from profile fitting of the Balmer lines in snapshot spectra. Taken at face value, for instance, the EW variations shown in Fig. 3 would translate in the most extreme cases into a $\pm$0.8 dex uncertainty in the derived mass-loss rate (Puls et al. 1996 equation 43). Although it remains to be seen whether a sophisticated modelling would result in drastically different figures, the large Hα changes intrinsic to the early-type supergiants may be one of the most important factors limiting the accuracy with which these objects can be used as extragalactic distance indicators (see discussion in Kudritzki 1999).

This survey has revealed the existence of cyclical Hα line-profile variations in HD 14134 and HD 42087. The low detection rate (two cases out of 17) may have several explanations, including observational limitations or a loss of coherency in the patterns of variability. HD 14134 is of particular interest, as it is one of the very few early-type stars clearly exhibiting the same pattern of variability in the photometric and spectroscopic modes. The existence of azimuthally structured outflows in our programme stars might explain the dramatic Hα changes, but firm conclusions must await detailed modelling (see Harries 2000, for the first effort in this direction). Sensitive searches for close companions (e.g. via long-baseline optical interferometric observations) are also needed to firmly rule out a variability arising from wind interaction.

We do not find evidence for a direct coupling between the wind activity and base perturbations arising from pulsations, but we

caution that our data are not well suited to examine this aspect in detail. It is conceivable that in several instances the globally anisotropic nature of the outflow primarily results from the putative existence of small-scale magnetic loops anchored at the stellar photosphere (or alternatively a presumably fossil, large-scale dipole field). A major observational effort is currently undertaken to detect such weak magnetic fields in early-type stars (e.g. Henrichs et al. 2003). Firm detections can be expected in the forseeable future. They would place the above conclusions on a quantitative footing and directly address the relevance of this scenario.

ACKNOWLEDGMENTS

This work is based on observations collected at the VBO, Kavalur, India. We are indebted to G. A. Wade and the TBL-MuSiCoS team for obtaining a single circular polarization spectrum of HD 14134 during the mission 'Precision Studies of Stellar Magnetism Across the HR Diagram' (2003 July). This work greatly benefited from the comments of the anonymous referee. The authors would like to acknowledge the support from the Applied Research and Technology Program at Western Kentucky University (WKU) and the assistance of the undergraduate telescope operators at WKU who participated in the observing programme: A. Atkerson, T. Monroe and W. Ryle. It is a pleasure to thank the staff of the VBO for their excellent support. We are also grateful to the VBO chairman for the generous allotments of observing time. We wish to thank A. F. J. Moffat for useful comments. This research made use of the National Aeronautics and Space Administration (NASA) Astrophysics Data System Bibliographic Services and the Simbad data base operated at Centre de Données astronomiques de Strasbourg (CDS), Strasbourg, France.

REFERENCES

Abt H. A., Levy S. G., 1973, ApJ, 184, 167
Abt H. A., Levato H., Grosso M., 2002, ApJ, 573, 359
Adelman S. J., Yüce K., Engin S., 2000, IBVS, 4946, 1
Antokhin I. I., Bertrand J.-F., Lamontagne R., Moffat A. F. J., Matthews J., 1995, AJ, 109, 817
Balona L. A., 1992, MNRAS, 254, 404
Berghöfer T. W., Schmitt J. H. M. M., Cassinelli J. P., 1996, A&AS, 118, 481
Bresolin F., Pietrzyński G., Gieren W., Kudritzki R. P., Przybilla N., Fouqué P., 2004, ApJ, 600, 182
Chalabaev A., Maillard J. P., 1983, A&A, 127, 279
Charbonneau P., MacGregor K. B., 2001, ApJ, 559, 1094
Cherrington E. F., 1937, ApJ, 85, 139
Conti P. S., Leep E. M., 1974, ApJ, 193, 113
Cranmer S. R., Owocki S. P., 1996, ApJ, 462, 469
de Jong J. A., Henrichs H. F., Schrijvers C., Gies D. R., Telting J. H., Kaper L., Zwarthoed G. A. A., 1999, A&A, 345, 172
de Jong J. A. et al., 2001, A&A, 368, 601
Denizman L., Hack M., 1988, A&AS, 75, 79
Donati J.-F., Semel M., Carter B. D., Rees D. E., Cameron A. C., 1997, MNRAS, 291, 658
Donati J.-F., Wade G. A., Babel J., Henrichs H. F., de Jong J. A., Harries T. J., 2001, MNRAS, 326, 1265
Donati J.-F., Babel J., Harries T. J., Howarth I. D., Petit P., Semel M., 2002, MNRAS, 333, 55
Ebbets D., 1980, ApJ, 235, 97
Ebbets D., 1982, ApJS, 48, 399
Eversberg T., Lépine S., Moffat A. F. J., 1998, ApJ, 494, 799
Feigelson E. D., Broos P., Gaffney J. A. III, Garmire G., Hillenbrand L. A., Pravdo S. H., Townsley L., Tsuboi Y., 2002, ApJ, 574, 258
Fullerton A. W., Gies D. R., Bolton, C. T., 1996, ApJS, 103, 475
Fullerton A. W., Massa D. L., Prinja R. K., Owocki S. P., Cranmer S. R., 1997, A&A, 327, 699
Grillo F., Sciortino S., Micela G., Vaiana G. S., Harnden F. R. Jr, 1992, ApJS, 81, 795
Harries T. J., 2000, MNRAS, 315, 722
Henrichs H. F., Kaper L., Nichols J. S., 1994, A&A, 285, 565
Henrichs H. F., Neiner C., Geers V. C., 2003, in van der Hucht K., Herrero A., Esteban C., eds, Proc. IAU Symp. Vol. 212, A Massive Star Odyssey: From Main Sequence to Supernova. Astron. Soc. Pac., San Francisco, p. 202
Herrero A., Puls J., Najarro F., 2002, A&A, 396, 949
Hinkle K., Wallace L., Valenti J., Harmer D., 2000, Visible and Near Infrared Atlas of the Arcturus Spectrum 3727–9300 Å. Astron. Soc. Pac., San Francisco
Howarth I. D., 2004, in Maeder A., Eenens P., eds, Proc. IAU Symp. 215, Stellar Rotation. Astron. Soc. Pac., San Francisco, in press
Howarth I. D., Prinja R. K., 1989, ApJS, 69, 527
Howarth I. D., Prinja R. K., Massa D. L., 1995, ApJ, 452, L65
Howarth I. D., Siebert K. W., Hussain G. A. J., Prinja R. K., 1997, MNRAS, 284, 265
Hummel C. A., White N. M., Elias II N. M., Hajian A. R., Nordgren T. E., 2000, ApJ, 540, L91
Humphreys R. M., MacElroy D. B., 1984, ApJ, 284, 565
Kaper L., 1998, in Wolf B., Stahl O., Fullerton A. W., eds, Proc. IAU Colloquium Vol. 169, Variable and Non-Spherical Stellar Winds in Luminous Hot Stars. Astron. Soc. Pac., San Francisco, p. 193
Kaper L., Henrichs H. F., Nichols J. S., Snoek L. C., Volten H., Zwarthoed G. A. A., 1996, A&AS, 116, 257
Kaper L. et al., 1997, A&A, 327, 281
Kaper L., Fullerton A. W., Baade D., de Jong J. A., Henrichs H. F., Zaal P., 1998, in Kaper L., Fullerton A. W., eds, Proc. ESO Workshop, Cyclical Variability in Stellar Winds. Springer-Verlag, Berlin, p. 103
Kaper L., Henrichs H. F., Nichols J. S., Telting J. H., 1999, A&A, 344, 231
Kaufer A., Stahl O., Wolf B., Gäng Th., Gummersbach C. A., Kovács J., Mandel H., Szeifert Th., 1996, A&A, 305, 887
Kaufer A. et al., 1997, A&A, 320, 273
Kaufer A., Prinja R. K., Stahl O., 2002, A&A, 382, 1032
Kiriakidis M., Fricke K. J., Glatzel W., 1993, MNRAS, 264, 50
Koen C., 2001, MNRAS, 321, 44
Krzesiński J., Pigulski A., Kolaczkowski Z., 1999, A&A, 345, 505
Kudritzki R. P., 1999, in Wolf B., Stahl O., Fullerton A. W., eds, Proc. IAU Colloquium Vol. 169, Variable and Non-Spherical Stellar Winds in Luminous Hot Stars. Astron. Soc. Pac., San Francisco, p. 405
Kudritzki R. P., Puls J., Lennon D. J., Venn K. A., Reetz J., Najarro F., MacCarthy J. K., Herrero A., 1999, A&A, 350, 970
Lamers H. J. G. L. M., 1981, ApJ, 245, 593
Lamers H. J. G. L. M., Cassinelli J. P., 1996, in Leitherer C., Fritze-von-Alvensleben U., Huchra J., eds, ASP Conf. Ser. Vol. 98, From Stars to Galaxies: The Impact of Stellar Physics on Galaxy Evolution. Astron. Soc. Pac., San Francisco, p. 162
MacGregor K. B., Cassinelli J. P., 2003, ApJ, 586, 480
Marchenko S. V. et al., 1998, A&A, 331, 1022
Markova N., 2002, A&A, 385, 479
Mason B. D., Gies D. R., Hartkopf W. I., Bagnuolo Jr. W. G., Brummelaar T. T., MacAlister H. A., 1998, AJ, 115, 821
Massa D. L. et al., 1995, ApJ, 452, L53
Mayer P., Hanna M. A., Wolf M., Chochol D., 1998, Ap&SS, 262, 163
Miller N. A., Cassinelli J. P., Waldron W. L., MacFarlane J. J., Cohen D. H., 2002, ApJ, 577, 951
Moffat A. F. J., Michaud G., 1981, ApJ, 251, 133
Morel T., Marchenko S. V., Pati A. K., Kuppuswamy K., Carini M. T., Wood E., Zimmerman R., 2004a, in Maeder A., Eenens P., eds, Proc. IAU Symp. Vol. 215, Stellar Rotation. Astron. Soc. Pac., San Francisco, in press
Morel T, . Marchenko S. V., Pati A. K., Kuppuswamy K., Carini M. T., Wood E., Zimmerman R., 2004b, BASI, in press
Owocki S. P., 1994, Ap&SS, 221, 3

Pamyatnykh A. A., 1999, Acta Astron., 49, 119
Petrenz P., Puls J., 1996, A&A, 312, 195
Prinja R. K., Massa D. L., Fullerton A. W., 1995, ApJ, 452, L61
Prinja R. K., Fullerton A. W., Crowther P. A., 1996, A&A, 311, 264
Prinja R. K., Massa D. L., Howarth I. D., Fullerton A. W., 1998, MNRAS, 301, 926
Prinja R. K., Stahl O., Kaufer A., Colley S. R., Crowther P. A., Wolf B., 2001, A&A, 367, 891
Prinja R. K., Massa D. L., Fullerton A. W., 2002, A&A, 388, 587
Puls J. et al., 1996, A&A, 305, 171
Reid A. H. N., Howarth I. D., 1996, A&A, 311, 616
Rivinius Th. et al., 1997, A&A, 318, 819
Roberts D. H., Lehár J., Dreher J. W., 1987, AJ, 93, 968
Rosendhal J. D., 1973, ApJ, 182, 523
Rufener F., Bartholdi P., 1982, A&AS, 48, 503
Rusconi L., Sedmak G., Stalio R., Arpigny C., 1980, A&AS, 42, 347
Ryans R. S. I., Dufton P L., Rolleston W. R. J., Lennon D. J., Keenan F. P., Smoker J. V., Lambert D. L., 2002, MNRAS, 336, 577
Scargle J. D., 1982, ApJ, 263, 835
Smith M. A., Ebbets D., 1981, ApJ, 247, 158
Stahl O. et al., 1996, A&A, 312, 539
Sterken C., Wolf B., 1978, A&A, 70, 641
Sterken C., de Groot M., van Genderen A. M., 1997, A&A, 326, 640
Thaller M. L., Gies D. R., Fullerton A. W., Kaper L., Wiemker R., 2001, ApJ, 554, 1070
ud-Doula A., Owocki S. P., 2002, ApJ, 576, 413
Underhill A. B., 1960, PASP, 72, 363
Underhill A. B., 1961, Pub. Dom. Ap. Obs. Victoria, 11, 353
van Genderen A. M. et al., 1989, A&AS, 79, 263
van Helden R., 1972, A&A, 21, 209
Waelkens C. et al., 1990, A&AS, 83, 11
Waelkens C., Aerts C., Kestens E., Grenon M., Eyer L., 1998, A&A, 330, 215
Waldron W. L., Cassinelli J. P., 2000, ApJ, 548, L45
Zeinalov S. K., Rzaev A. Kh., 1990, Ap&SS, 172, 217

This paper has been typeset from a TEX/LATEX file prepared by the author.